International Journal of Disaster Risk Reduction 19 (2016) 311–323

Contents lists available at ScienceDirect

International Journal of Disaster Risk Reduction

journal homepage: www.elsevier.com/locate/ijdrr

Multi-hazard risk assessment of two Hong Kong districts

Katie Johnson [a,b,*], Yaella Depietri [c], Margaretha Breil [a,b]

[a] Fondazione Eni Enrico Mattei (FEEM), Isola San Giorgio Maggiore, 30124 Venice, Italy
[b] Euro-Mediterranean Center on Climate Change (CMCC), Isola San Giorgio Maggiore, 30124 Venice, Italy
[c] Urban Ecology Lab, Environmental Studies Program, The New School, 79 Fifth Avenue, 16th Fl., New York, NY 10003, USA

ARTICLE INFO

Article history:
Received 3 May 2016
Received in revised form
28 August 2016
Accepted 29 August 2016

Keywords:
Urban areas
Hazard
Vulnerability
Risk
Climate change
GIS

ABSTRACT

The assessment of multi-hazard risks in urban areas poses particular difficulties due to the different temporal and spatial scales of hazardous events, and the potential interactions between hazards and socio-economic fragilities. Yet this exercise is important, as identifying the spatial distribution and concentration of risks in urban areas helps determine where and how preventive and corrective actions can reduce levels of vulnerability and exposure of urban populations. This article presents the results of a GIS-based assessment of present day risk to socio-natural hazards in two socio-economically distinct districts of Hong Kong (PRC) by utilizing indicators to describe the hazards and vulnerabilities. Hong Kong is a densely populated coastal metropolis exposed to multiple intense and potentially overlapping hydro-meteorological hazards, including heat waves, typhoons, and landslides. Mapping hazards and vulnerabilities in this urban area helps to visualize the spatial distribution and concentrations of risk located throughout the city, and thereby facilitate the tailoring of measures that can reduce risk at the very local scale. This approach has the potential of providing city planners and policy makers with visual guidance in prioritizing risk management and adaptation actions with respect to current and future risks existing in specific parts of the city, taking into account more than one hazard at the time. We found that the two districts considered have comparable and distributed levels of risk being both exposed to multiple hazards and notwithstanding the socio-economic groups. However, elements of criticality are potentially more widespread in the less wealthy parts of the city.

1. Introduction

Natural hazards in the Asia-Pacific region affected 6 billion people and caused over 2 million casualties between 1970 and 2014 [1]. These fatalities and the number of persons affected represent a significant portion of the worldwide totals: according to the Economic and Social Commission for Asia and the Pacific, 56.6% of the deaths and 87.6% of people affected due to hazards, especially hydro-meteorological ones, are located in this region. While the total number of fatalities per disaster has actually decreased over the past several decades, economic damages have increased [1]. Disaster risk reduction (DRR) activities have helped to lower the number of deaths, yet factors including population growth, development of cities in coastal areas, and climate change contribute to increased exposure and damages. Since 1980 the number of people exposed to hydro-meteorological hazards, like floods and storms (cyclones), has increased by 70% [2], and this number is likely to rise with population growth and climate change. Indeed, Asia's urban population is projected to increase from 2.06 billion in 2014 to 3.31 billion in 2050 [3] further increasing the number of people exposed to natural hazards. Urban centres in the Asia-Pacific region are often located in geographically vulnerable areas, and development, especially of land occupied by the urban poor, is increasingly occurring in hazard-prone areas [1]. A large portion of Asia's urban population (238 million in 2000) lives less than 10 m above sea level [4], highly exposed to storm surges and sea level rise.

The concentration of people, infrastructures, and assets leave urban areas at a greater risk to suffering fatalities and economic losses from natural hazards compared to rural areas [5]. Heat waves are compounded by the Urban Heat Island (UHI) effect and air pollution [see for instance, [6]], and impacts of coastal, river and flash flooding are enhanced by the high presence of sealed surfaces [see for instance, [7]]. DRR is rarely included in plans for rapid urban expansion worldwide [2] as the two communities often consider their tasks as separate. Spatial and institutional competences do not coincide in most cases, and space constrictions and socio-economic conditions frequently drive urban expansion into hazard prone areas [8].

* Corresponding author at: Fondazione Eni Enrico Mattei (FEEM), Isola San Giorgio Maggiore, 30124 Venice, Italy.
E-mail addresses: katie.johnson@feem.it (K. Johnson), depietry@newschool.edu (Y. Depietri), margaretha.breil@feem.it (M. Breil).

http://dx.doi.org/10.1016/j.ijdrr.2016.08.023
2212-4209/

This paper develops an indicator based approach for the spatial assessment of the risk to multiple hazards (i.e. heat waves, landslides, and storm surges) in two socio-economically diverse districts of Hong Kong Special Administrative Region of the People's Republic of China (herein referred to as Hong Kong). It applies strategies that can improve the knowledge needed for managing and reducing disaster risks in urban areas, with some consideration in the case of future climates. Section 2 provides the state of the art concepts, methods and background information on multi-hazard risk assessment. Section 3 presents the case study areas and the features of several hazards for Hong Kong; Section 4, the methodology used; Section 5, the results; Section 6, the final discussion; and Section 7, the conclusions.

2. Hazard, risk, and vulnerability: concepts and methods

The terms "hazard," "risk," and "vulnerability" are often defined in a slightly different manner from one scientific community to another. Whereas the climate change community focusses on impacts potentially causing hazards, knowing that impacts can be addressed by climate change mitigation and certain measures can reduce vulnerability, the contribution of the socio-economic system to the conformation of hazards has more gradually entered in the focus of the hazard risk community.

One current characterization of risk is based on the combination of the probability or likelihood of a natural hazard occurring and the vulnerability of the system potentially affected [9]. This definition, utilized by The United Nations Office for Disaster Risk Reduction (UNISDR), is the result of an increasing convergence between the risk and the climate change communities. It explicitly includes the vulnerability of the interested parts of the socio-economic system, and implicitly refers to the potential direction for climate change adaptation action.

In the past several decades, the common approach to disaster risk management has shifted from characterizing the hazard and hazard frequencies, necessary for the design of relief action, towards a more vulnerability or prevention-oriented approach [see for instance, [10]]. The concept that the fragilities of the exposed and eventually impacted social-ecological system also contribute to risk is made evident, for instance, in the case where one hazard unevenly impacts distinct parts of the same city due to the socio-economic disparities [11]. This perspective extensively frames the concept and analysis of vulnerability in the climate change community [12], which has defined vulnerability as the "propensity or predisposition to be adversely affected," [13] encompassing characteristics of the system's exposure (*character, magnitude, and rate of climate change and variation to which a system is exposed*), sensitivity, and capacity to cope. Further to the capacity to cope, the capacity of the system to preventively reduce risk to hazards is called adaptive capacity, which governs "the ability of systems, institutions, humans, and other organisms to adjust to potential damage, to take advantage of opportunities, or to respond to consequences," [13]. In this sense, adaptive capacity is an element modifying vulnerability by enhancing the capacity to cope or by reducing exposure to climate change impacts in the long term.

The vulnerability perspective presents hazards not as inevitable events "naturally" affecting socio-ecologic systems, but as the result of the interaction between the features of the affected system and the event. The interaction that takes place between the natural and the social systems, determining a particular configuration of risk, develops not only on the characteristics of the hazard itself, but also on the conditions of the social-ecological system impacted. This perspective on the role of conditions of socio-economic systems opens a perspective on strategies for DRR that focus on the reduction of socio-economic causes of vulnerabilities. UNISDR, similar to the IPCC [14], defines socio-natural hazards as those where "the causes are a combination of natural and anthropogenic factors, including environmental degradation, climate change and others" [9]. This perspective further helps in identifying the multiple causes of risk, moving away from the inevitability of the damages occurring to the impacted system. For example, this is the case with the concentration of air pollution or the UHI effect, both increasing the impacts of heat waves in cities [15], or of the poor living in areas that are more exposed to disaster risks, like river and coastal floodplains or steep slopes and areas at risk of landslides, which is true for cities in the developing world as well as for those in developed countries [16,17].

2.1. Multi-hazard risk in urban areas

Hazards can affect differently people and infrastructures of a single urban system. The impacts can concentrate spatially, affecting some parts of the city more than others. Furthermore, socio-economic elements of vulnerability are normally distributed in an uneven manner across urban areas, generating, from a spatial point of view, a concentration of or overlap of different risks. Already in the early nineties, the consideration of multiple risks was proposed as part of the requirements for the definition of strategies for sustainable urban development, for instance as part of Agenda 21 for sustainable development [18], and was reconfirmed in the Johannesburg Declaration of Sustainable Development in 2002, which required "[a]n integrated, multi-hazard, inclusive approach to address vulnerability, risk assessment and disaster management, including prevention, mitigation, preparedness, response and recovery," [19]. In a similar manner, the Hyogo Framework of Action pledged for the mainstreaming of "integrated, multi-hazard approach[es] for disaster risk reduction […] into policies, planning and programming" [20], and the Sendai framework reiterated the same message explicitly calling for "comprehensive surveys on multi-hazard disaster risks" [21].

The concentration of risks in urban areas derives from a set of different and often overlapping sources of vulnerabilities and hazards. This variety of hazards concentrated in a relatively small space makes multi-hazard assessment an increasingly important yet challenging task for DRR in cities for several reasons. First, various hazards have different characteristics, their impacts on structures and buildings are diverse, however they can potentially act at coinciding scales in space and time (e.g. frequencies, times of onset, as well as durations) [22–24]. Second, the socio-economic conditions determining vulnerabilities are not distributed evenly in urban areas. The dense and interconnected structures of cities create strong spatial differentiations. These factors represent a challenge for the analysis and assessment of urban disaster risks as they impose the use of diversified approaches [25–28]. In particular, the methods available for the description and quantification of single risks needs to be adapted carefully to the contemporary or comparative assessment of multiple risks [23,29].

A basic approach to multi-hazard mapping consists in the mapping of "the totality of relevant hazards in a defined area" [30]. This implies defining the urban areas potentially exposed to hazards. Such an approach allows for the identification of potential hotspots of vulnerability, where more than one potential hazard can have impacts, providing specific indications for disaster preparedness [see for instance,31]. Under this perspective, the effects of hazards are considered simply additive, with overlapping impacts. A more sophisticated approach would consist in relating the spatial or causal interactions between different hazards and analysing the relative importance of single impacts [27]. Another issue worth considering is that of interrelated hazards, as hazards frequently occur as consequences of other types of hazards (e.g. landslides provoked by seismic events or chemical incidents by flooding), or alongside them (e.g. cloud burst events causing both flooding and landslides in the same or contiguous urban areas) [32].

Interacting hazards can be compound hazards: under a spatial approach, the simple fact that two different hazards impact the same people or the same elements of the urban system can cause effects that go beyond the sum of single independent impacts [27]. Impacts acting on the same parts of the territory, without interacting causally or coinciding contemporaneously, may need to be considered jointly as measures for reducing risks to one impact might enhance vulnerabilities towards other hazards, thereby accentuating hotspots of vulnerability.

The different options for spatial and temporal interactions, as presented by Kappes et al. [30], have diverse implications in terms of potential forms of action in the urban domain. In the case of spatial but not temporal coincidence of impacts, measures for risk reduction should aim to reduce risks from the single hazards, taking into account the co-presence of them all (e.g. measures taken to lessen the impact of heat need not compromise safety in cases of floods or landslides). In the case of spatially and temporally coinciding hazards, further to impacts from single hazards, results from interaction and cascading effects need to be taken into account. Finally, the case of simultaneous but not spatially coinciding hazards represents a challenge in terms of risk and emergency management, as in different parts of the city, different types of emergency situations will require different types of management intervention at the same time [following [30]].

From an assessment point of view, the consideration of multiple hazards requires the creation of complex spatial indices, which provide aggregated information about risks from different hazards alongside with exposure and aspects of sensitivity and coping capacity for single parts of the urban area. In this sense, single indicators and aggregated indices represent a synthetisation of a complex reality and represent phenomena that, as for instance with vulnerability, are difficult or impossible to measure. Spatial interactions can be captured, inter alia, by simply summing up single hazard indices to create an overall urban multiple hazards map. Using an additive approach for the aggregation of spatial indices for hazards has the disadvantage of hiding potential compensative effects between high and low risk levels across different hazards. Furthermore, additive approaches do not detect (eventual non-linear) interaction between the hazards and the system, which can cause changes in the characterization of the hazards themselves (e.g. cloud bursts or inundation can combine in unforeseen way with coastal flooding and slope instability) and in changes in the state of the urban system. The changes can cause new and different types or forms of risk which are different from the sum of single hazards, leading to important underestimations of risk [29], although interactions between more than one hazard are still not well understood [30,32]. Despite the limitations, the approach still retains the potential to allow for the identification of hotspots of hazard exposure. Further to the consideration of interactions, a multi-hazard approach needs to establish metrics which make risks comparable. Classification offers a simple approach to compare risk [27] and semi-quantitative index based approaches have been developed by Dilley et al. [33], Greiving [34] and Greiving et al. [32]. These compute hazard and vulnerability separately and weight the hazard with the vulnerability index to calculate risk.

A further issue for comprehensive treatment of the hazards is connected to the aggregation of single indices. Several approaches for the aggregation of single indices are proposed in literature. For example, Greiving [34] proposes an integrated risk matrix with 10 degrees of risk obtained by summing vulnerability and hazards classes. The Global risk index is also calculated as the product of exposure (the hazard sphere) per susceptibility, coping capacity, and adaptive capacity [35]. Others have defined vulnerability spatially as the product of hazards features, sensitivity, and adaptive capacity [36] – what is referred to as risk herein. Carreño et al. [37] also assessed the risk to multiple hazards spatially in an urban context as a product of the potential physical damage (D), based on the exposure and an impact factor (I), aggregating susceptibility and lack of resilience of the exposed population. By multiplying D and I Carreño et al. [37] obtain a spatially explicit map of different risk at the district level.

Qualitative approaches have been applied by Granger et al. [38] and Middelmann and Granger [39], and a spatial multi-hazard assessment with qualitative weightings is also presented in El Morjani et. al. [40]. In this last health risk oriented study, different hazards are weighted according to the damages caused in past events. The regional averages of damages (persons killed or affected and economic damages) are expressed in monetary terms [40].

For a more in-depth review of multi-hazard assessment methods refer to Kappes et al. [27].

3. Hong Kong

Hong Kong is situated on the southern coast of China, close to the Pearl River Estuary and shares its northern border with Guangdong Province of Mainland China. Due to the particular socio-political position held by the city throughout the second half of the 20th century, Hong Kong has become one of the most densely populated areas of the world with around 6300 people per square kilometre. In 1841 the area only had about 7450 inhabitants [41], whereas in 1941 population was 1.64 million, dropping to 600,000 after World War II, growing to 3 million in 1960 [41], and finally reaching approximately 7.3 million inhabitants in 2015, according to the government census. The population is projected to increase at a rate of 0.6% to reach 8.47 million in 2041, and to continue ageing [42]. The population aged 65 and over is projected to grow from 13% in 2011 to 30% in 2030 [42].

The territory of Hong Kong is subdivided in eighteen districts, each of which consists of a variable number of constituencies. There are pronounced differences in terms of socio-economic conditions throughout different areas of the city in terms of income and living conditions. Further to statistical income levels, these differences are visible also with respect to the percentage of green areas and the environmental conditions across the city.

3.1. Central and Western District and Kwun Tong District

To perform a detailed analysis of multi-hazard risk at the very local level of the constituency, two of Hong Kong's eighteen districts are considered: Central and Western District and Kwun Tong District (see Fig. 1). They were chosen to capture a range of distinct socio-economic and environmental characteristics in coastal areas that are currently experiencing multiple hazards, such as storm surges, heat waves, and landslides. Specifically, the Central and Western District features as a high income level and low densities of residential population, and the Kwun Tong District shows a lower income level and a high number of inhabitants and population density. According to the 2011 Hong Kong Population Census, Kwun Tong District has the second largest population and the highest population density of all Hong Kong districts. Central and Western District is the third least populated and the eight densest district. Kwun Tong has the sixth highest median age, and Central and Western the twelfth highest. Extensive waterfronts characterize both districts. Central and Western District, which has a dense central business district situated along the coast, covers an area of about 1255 ha and is broken down into 15 constituencies in the

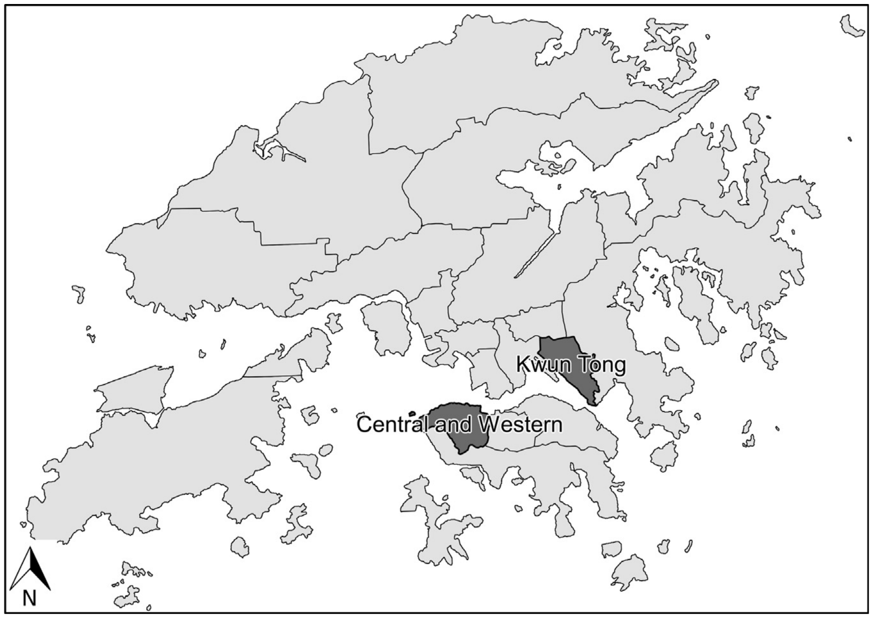

Fig. 1. Map of Hong Kong highlighting Central and Western District and Kwun Tong District.

Table 1
Socio economic indices of the study areas.

	Hong Kong	Central and Western	Kwun Tong
Surface (km^2)	1104	12.52	11.05
Population	7,071,576	251,519	622,152
Population density (people/ km^2)	6405	20,089	56,303
Median age	41.7	41.3	42.8
Median monthly income (HKD)	11,000	15,000	10,000
Population change 2001–2011 (%)	5.4	−4	10.6

Data source: Hong Kong Population Census 2011 [87].

2011 census. Kwun Tong District is slightly smaller at around 1130 ha, and is divided into 35 constituencies according to the 2011 census. See Table 1 for socio-economic indices of the study area.

Figs. 2 and 3 serve as a reference for the names associated with each constituency area in Central and Western District and Kwun Tong District.

3.2. Natural hazards

Hong Kong is situated along the southeast rim of the Asian Pacific region, in an area that is especially exposed to strong typhoons (high wind and heavy precipitation) causing storms and floods.Tsunamis triggered by earthquakes are a second potential source of coastal flooding. Landslides often occur due to the steep slopes in mountainous parts of the city, triggered by heavy precipitation, especially during cyclones. As a densely urbanized area situated in a humid subtropical climate, Hong Kong is also affected by heat stress [43]. Although overall hazard preparedness has improved in Hong Kong in the last decades [44], there are substantial differences among age groups: a 2012 study revealed, for instance, that only 22.4% of the elderly were prepared for disasters [45].

3.2.1. Heat waves

The Hong Kong Observatory (HKO) has been recording the occurrence of very hot days and hot nights since 1884 (excluding the period of 1940–1946). Over this period, a total of 1031 days with a maximum temperature greater than or equal to 33 °C and

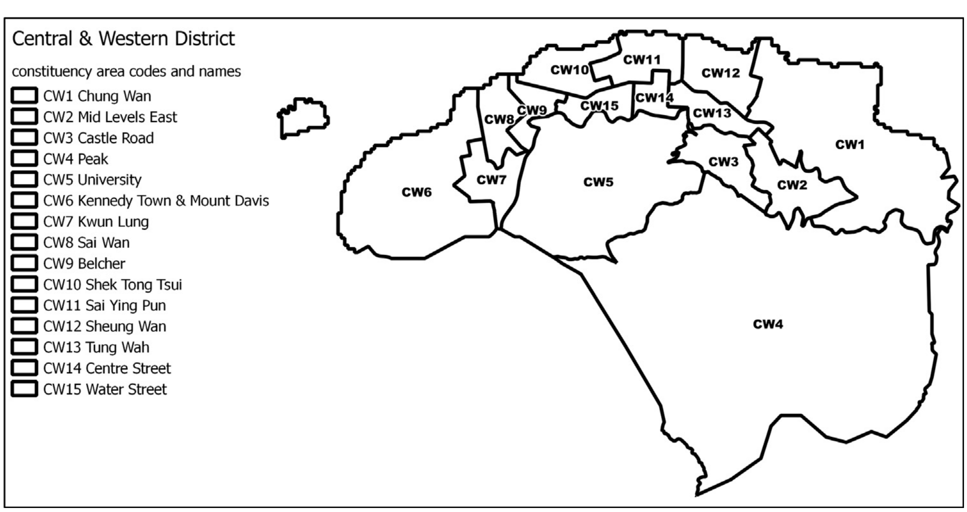

Fig. 2. Central and Western District's constituencies' areas.

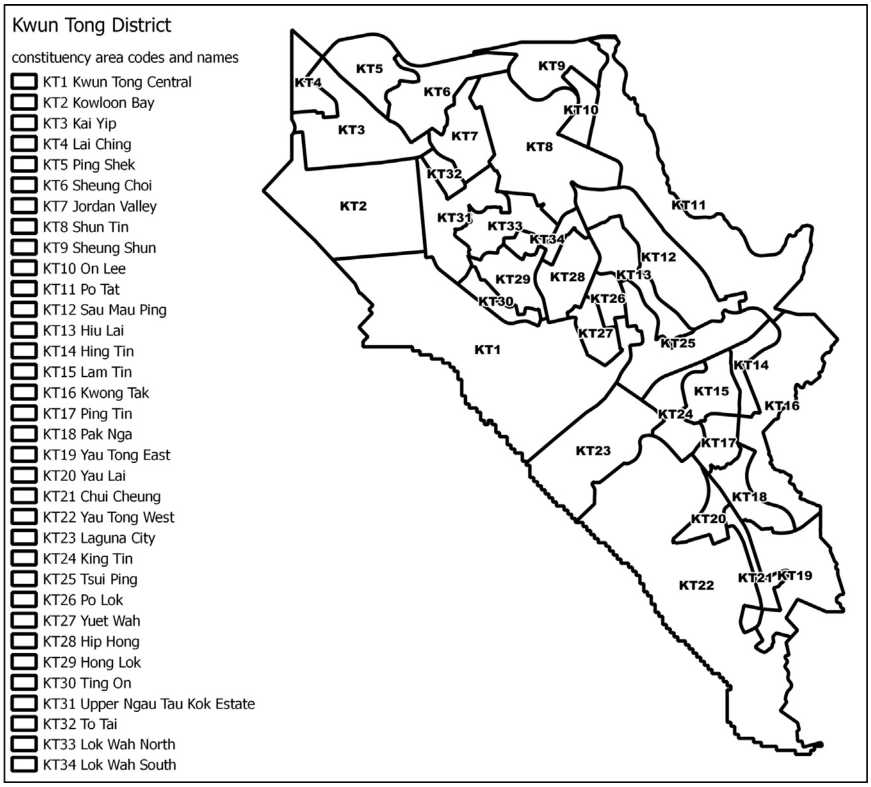

Fig. 3. Kwun Tong District's constituencies' areas.

894 nights with a minimum temperature greater than or equal to 28 °C have been recorded.

Since 2000, the HKO has been issuing Very Hot Weather Warnings (VHWW) to alert the population in the event of a heatwave. Warnings are generally issued when temperature reaches 34 °C, or exceeds 30 °C together with a certain humidity level, wind speed and direction. Between January 2000 and October 2015, the VHWW was issued 203 times; the average duration of each very hot weather event was about 1.5 days.

These hot conditions represent a particular risk, especially for elderly people living alone, and in the case of long spells [44] (more than 3 consecutive days). Currently there are 14 heat shelters in Hong Kong managed by the Home Affairs Department that opened in the summer 2007 [46]. The city around the delta is also affected by high levels of air pollution favoured by the high density of tall buildings. However, daily mortality connected to air pollution seems to be higher in the cool season in correspondence with northeast monsoons than in the warm one [47–49]. Episodes of high concentration of Ozone (O_3) and Particulate Matter smaller than 10 μm (PM_{10}) have been recorded during the hot season, linked to the presence of tropical cyclones and originating from sources of pollution located at the regional level [50,51]. In combination with heat waves, this might nonetheless contribute to the number of excess deaths in extreme hot weather conditions, as suggested by Chau et al. [46].

3.2.2. Typhoons

Hong Kong's typhoon season spans from May to November, peaking during the summer months of June, July, and August. These tropical cyclones often result in flooding and landslides [52]. In the past, the greatest death toll and economic losses have been inflicted by typhoon-induced storm surges [44,53]. According to the HKO's database on Storm Surge Records in Hong Kong during the Passage of Tropical Cyclones from 1949 to 2015, tide gauges nearby the case study areas have recorded water levels as high as 1.77 m above the astronomical tide.

In the city's history, typhoons are the hazards that have caused the most casualties and damages in Hong Kong [44]. According to the International Disaster Database (EM-DAT), in 1906 a tropical storm hit the city causing 10,000 deaths while another typhoon caused 11,000 deaths in 1937. In 1947, 2000 people died in a storm. In June 1960, Typhoon Mary hit the city affecting more than 15,000 people. According to EM-DAT, floods too are at the origin of high numbers of people affected in Hong Kong, and together with storms cause the highest amount of economic damages. On the other hand, typhoons and cyclones also bring benefits to Hong Kong. Cyclones are responsible for at least 30% of annual rainfall in the area, and are therefore important for the water balance of the city, also by breaking drought periods and cooling the environment [54]. The downside is that these precipitation events are often concentrated in relatively short time periods. May, June, July, August, and September each have monthly rainfall levels exceeding 300 mm; about 80% of the yearly rainfall occurs in these 5 months. HKO monthly mean precipitation data from 1981 to 2010 indicates that June is the rainiest month in terms of both total and duration of rainfall.

The HKO issues Tropical Cyclone Warning Signals in the event of a typhoon. Warnings to the public are issued in case of persisting strong winds, storms, and in the case of tropical cyclones centered within 800 km of Hong Kong that may affect the city. From January 1964 to October 2015, 1028 cyclone warnings of signal 1 or higher were issued with an average duration of nearly 17 h.

3.2.3. Landslides

Landslides in Hong Kong have been studied in particular on the little inhabited Lantau Island [53,55–58]. Other researchers have looked at the New Territories district [58], and Hong Kong Island

[59]. Research on Hong Kong Island has found elevation to be the most dominant factor in explaining landslide occurrence in the area, whereas other research shows that the other factors, like slope angle, soil characteristics, and coverage might have a more important role [60,61]. Hong Kong Island is also more affected by landslides than the other parts of the city as it is the most populated area with high rates of soil sealing and high building densities [59].

Since 1983, the HKO and Geotechnical Engineering Office has been issuing landslip warnings when there is a high risk of landslips as a result of persistent heavy rainfall. Relevant government departments and organisations are prompted by warnings to take appropriate actions, including opening temporary shelters, standing by for search and rescue operations, and closing individual schools and relief work projects. From January 1983 to October 2015, a total of 103 landslip warnings was issued in Hong Kong.

4. Risk assessment methodology

Risk is defined by the likelihood of the system to be affected and is generally obtained by multiplying vulnerability indices with those describing the features of the hazards. Applying a comprehensive approach to the consideration of urban risks is functional to integrated urban policies that are able to address the spatial concentration of risks acting on morphological, socio-economic, and environmental roots of sensitivity, susceptibility, and lack of coping capacity.

The methodology applied in this spatially explicit multi-hazard risk assessment has been informed by the multi-risk assessment of Europe's regions described in Greiving [34], opting for a linear aggregation rather than a multiplicative approach of final indicators for each of the hazard specific risks. The methodology consists of four steps: (1) developing intensity maps for each socio-natural hazard based on a set of clearly identified indicators using normalized indices in order to keep values based on different dimensions and metrics comparable (see Table 2); (2) deriving an integrated hazard map encompassing and overlaying all the hazards considered; (3) developing a vulnerability map based on the indicators of exposure, sensitivity, and adaptive capacity (see Table 3) relevant for the hazards considered; and (4) obtaining an integrated risk map as a product of the values of the multi-hazards map and of the vulnerability map.

Thus we begin here with an analysis of all single hazards and their impacts, with special attention given to potential interactions with contemporaneous or sequential hazards: those in which one process triggers the next or those in which the disposition of one hazard is altered by another (e.g. earthquake induced landslides, or floods and landslides triggered by extreme rainfall or coinciding with river or coastal flooding) [62,63]. For each of the single hazards considered, indicators that could be mapped using the available information have been chosen. With regard to interactions, the spatial overlay of these single indicators in multiple hazard maps provides a first idea on the existence of eventual interactions.

Table 2
List of descriptors of spatial intensity of the socio-natural hazards considered.

Hazard (*H*)	**Indicator/parameter**	**References**
Heat waves (*HW*)	UHI: sealed surface area (excluding buildings, *SSA*) plus building volume (*BV*)	[65–68]
Landslides (*L*)	Slope area: percent of land area with steep slope (higher than 45 degrees) (*SA*)	[60,61]
Storm surges (*SS*)	Floodable area: percent of land area below highest observed storm surge water level	[68,69]

Next, the sensitivities of the single elements exposed to the multiple hazards and determine degrees of risk are examined one by one. These are comparable across different hazards that are not expressed by a common metric system, provided that hazards are analyzed on the same spatio-temporal scale and on the same risk metric (economic, ecological or social, etc.) [29], using a classification approach based on a semi-quantitative index following Dilley et al. [33], Greiving [34] and Greiving et al. [32].

Finally, results are aggregated. Greiving et al. [32] presents a qualitative Integrated Risk Index (IRI) as basis for spatial planning decisions, which is based on the aggregation of single components of risk. The intensity of single hazards (or hazard impacts) relevant for spatial planning are classified into five intensity classes and aggregated into an integrated hazard risk component. In the present study, the two composite indicators for multi-hazard and vulnerability are equally weighted for the creation of the integrated risk maps [32]. An in-depth consideration of the results for urban planning in the city context would however require the application of specific weights based on local expert judgements.

All mapping was done using QGIS software [64].

4.1. Socio-natural hazard assessment

The heatwave hazard is estimated using the indicator for the UHI effect. As a hazard determined by socio-economic factors like urban density that exacerbate the impacts of natural hazards like heat waves, a combined index based on the percentage of sealed surface area and building volume is used. As mentioned, it is assumed that heatwaves impact the entire city, and the intensity of the hazard is a function of the UHI phenomena.

The landslide hazard is estimated using the percentage of the constituency with a slope greater than 45 degrees. This threshold is chosen as landslides generally occur on steeply sloped lands. Due to lack of data on soil characteristics and soil coverage, only the slope inclination could be used for this assessment. Landslide distribution data for 428 cut-slope failures on Hong Kong Island shows that most landslides occurred in areas with an inclination from 55° to 60°; other landslide data are distributed around this value in a form of normal distribution [61].

Floodable area is the most relevant factor composing the storm surge hazard, so the percentage of the constituency area between sea level and the highest observed storm surge water level from 1949 to 2015 is used to estimate the storm surge hazard.

For both districts, the intensities of impacts from hazards are assessed spatially, while the time dimension is excluded due to lack of available information.

$$H = (1/3HW) + (1/3L) + (1/3SS) \tag{1}$$

where H is integrated hazard, HW is heat wave, L is landslide, and SS is storm surge.

The individual hazards have been calculated taking into account single features of the urban system contributing to the specific risk:

$$HW = UHI = (1/2SSA) + (1/2BV) \tag{2}$$

where *SSA* is the sealed surface area and *BV* is the building volume.

$$L = (1/2SA) \tag{3}$$

where *SA* is the percent of land area with a slope greater than or equal to 45 degrees.

$$SS = \text{percent of land area below the highest observed storm surge water level} \tag{4}$$

Table 3
List of indicators describing the multi-hazard vulnerability of Hong Kong.

Vulnerability component	Indicator	References
Exposure (*E*)	Constituency population (as a percent of Hong Kong's total population)	[70]
Susceptibility (*S*)	Young people (percent population < 5) (*Y*) and Elderly (percent population > 65) (*A*)	[47–49,71,72]
	Unemployed (percent) (*U*)	[73]
	Income (median monthly domestic household income) (*I*)	[74,75]
	Education (percent of population over 15 with max primary level of education) (*P*)	[76–80]
Lack of coping capacity (*LCC*)	One person households (percent of households)	[49,80–82]

Each indicator of hazard is classified into five classes applying the equal intervals method in order to facilitate the comparison of constituencies in the districts in terms of heat waves, landslides, storm surges, and integrated hazard.

The primary source of land use data is the Hong Kong Survey and Mapping Office. The iB5000 Digital Topographic Map provides information on building footprint, land cover, and places of interest. This data is supplemented with Open Street Map data on leisure and natural areas in order to develop a more complete view of land use, particularly green areas.

High resolution LiDAR Digital Elevation Model (DEM) and Digital Surface Model (DSM) data are used in the assessment to derive information on elevation, slope, and building height. Data for Central and Western and Kwun Tong districts were provided by the Civil Engineering and Development Department. DEM and DSM data have a vertical accuracy specification of ± 0.10 m standard error (95% confidence level or 2σ) and a horizontal accuracy specification of ± 0.30 m standard error. DEM and DSM LiDAR data were collected from December 2010 to January 2011.

Tide gauge data is taken from the Hong Kong Observatory's database on Storm Surge Records in Hong Kong during the passage of tropical cyclones. Data from both Quarry Bay, collected from 1986 to 2015, and North Point, from 1949 to 1985, are considered as they are the tide gauges located closest to Central and Western District and Kwun Tong District.

4.2. Vulnerability assessment

Based on the literature and on data availability, a range of indicators has been chosen to characterize vulnerability to the different hazards. All indicators describe some aspects of the social-ecological system regarding its exposure, susceptibility, or coping capacity with respect to the potential hazards impacts. The indicators selected are presented in Table 3. While the inclusion of additional indicators would be desirable, especially in the case of lack of coping capacity where only one indicator is used, it is not feasible due to data limitations at the very local level of this assessment.

Socio-economic data used in the assessment has been obtained from the 2011 Hong Kong population census made available by the City Census and Statistics Department. Specifically, data on population, age, education, employment, income, people per household, and gender are considered for the 15 constituency areas within the Central and Western District on Hong Kong Island, and the 35 constituency areas within the Kwun Tong District in Kowloon. This data did not provide sufficient information for adequately assessing coping capacity, so the number of one person households was taken as a proxy for potential problems in coping of persons with specific needs not being sufficiently integrated in social networks.

4.2.1. Calculating vulnerability

Based on the definition of vulnerability, which is a function of exposure, susceptibility, and lack of coping capacity, socio-economic data has been normalized in order to assess relative differences in vulnerability between the districts and across constituencies. For population and income, normalization is done relative to all Hong Kong constituencies, whereas for the other variables it is done across the constituencies included within the two case study districts. Vulnerability, which exists only in areas where the population is exposed to hazards [83], is calculated as follows:

$$\mathrm{V} = \mathrm{E}*(S + LCC) \tag{5}$$

where *E* is exposure, *S* is susceptibility, and *LCC* is lack of coping capacity.

$$E = \text{constituency area population as percentage of Hong Kong's population} \tag{6}$$

$$S = (1/5Y) + (1/5A) + (1/5U) + (1/5I) + (1/5P) \tag{7}$$

where *Y* is the percentage of the population under age 5, *A* is the percentage of the population over age 65, *U* is the percentage of the population that is unemployed, *I* is income, and *P* is the percentage of the population over 15 years old with a maximum level of primary education.

$$LCC = \text{percent one person households} \tag{8}$$

Risk (R) is calculated as the product of hazard (H) and vulnerability (V):

$$R = H*V \tag{9}$$

5. Results

Figs. 4–8 report the results of the procedure depicting single hazards, integrated hazards, and the components of vulnerability, vulnerability, and risk. For a visual representation of the indicators, the levels of hazard, vulnerability, and risk are categorized into 5 classes based on the equal interval method of classification.

5.1. UHI, storm surge, and landslide hazards

Due to the densely populate area of Kwun Tong, the highest UHI effect is recorded for the Centre Street constituency of this district. Also, the heat wave impacts are aggravated in some of the inland constituencies of Central and Western District (Fig. 4a). The coastal constituencies of both districts present the higher level of storm surge intensity with slightly higher levels in Kwun Tong District (Fig. 4b). With respect to landslides, the internal constituencies of Central and Western District appear to be the most likely to be affected by the hazard (Fig. 4c). Overall the different hazards affect the constituencies in a rather complementary manner and with spatial overlap between the heat waves and storm surge hazards.

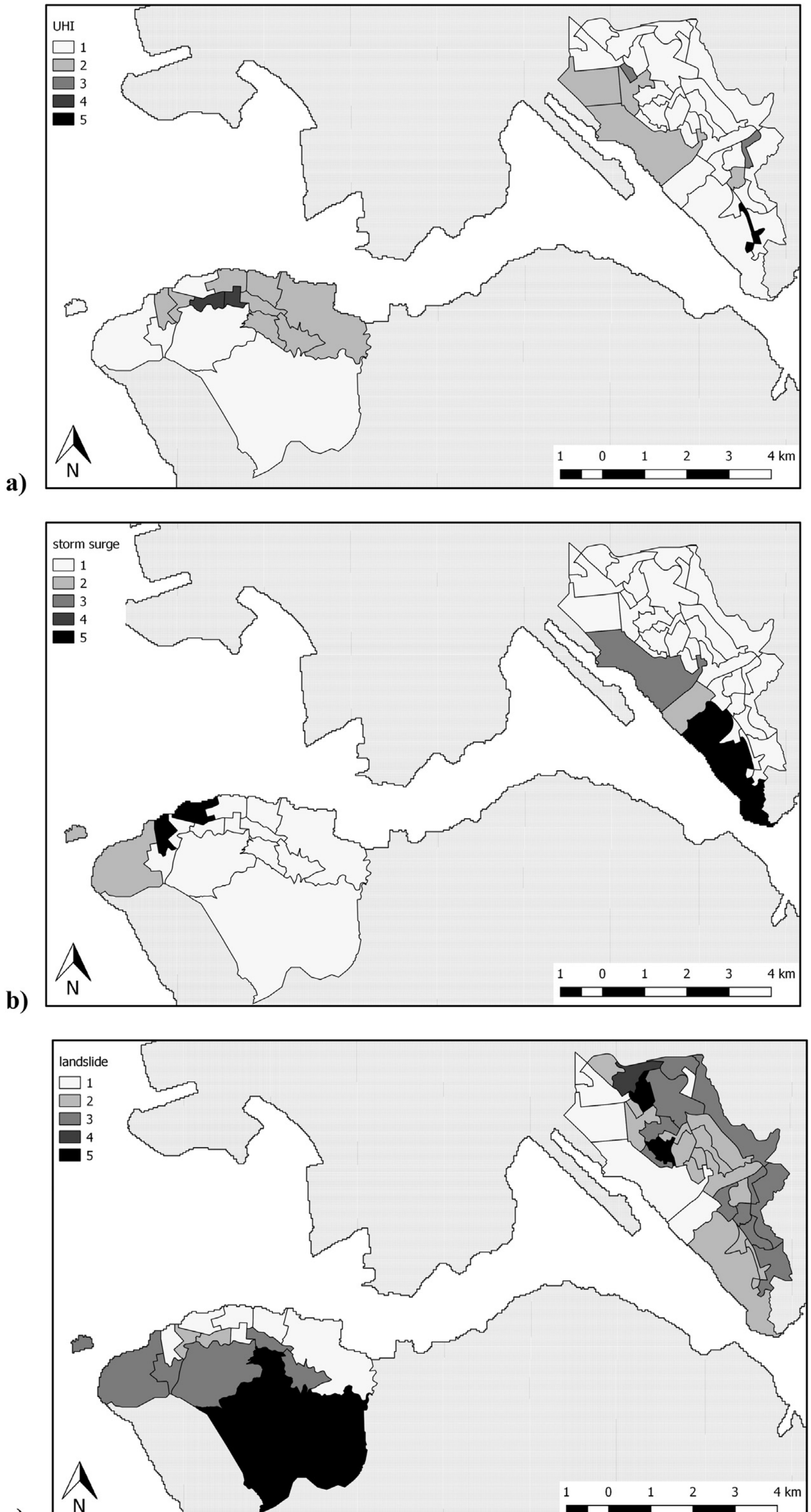

Fig. 4. (a) UHI, (b) storm surge, and (c) landslide hazards maps for Central and Western District (left) and Kwun Tong District (right).

5.1.1. *Integrated hazards*

The resulting multi-hazard map (Fig. 5) shows that close to none of the constituencies of the two districts are hazard free and that hazards are all distributed across all of the constituencies with comparable levels between the two districts. However, most constituencies of Central and Western District would suffer the highest multi-hazard impacts (i.e. close to half are in class 4 or 5) while in Kwun Tong most of the constituencies present a multi hazard risk level of only 2.

5.2. *Vulnerability*

As the population is well distributed across all of the constituencies, these show relatively low degrees of exposure if compared with the constituency Sau Mau Pang in Kwun Tong, which represents by far the highest concentration of population

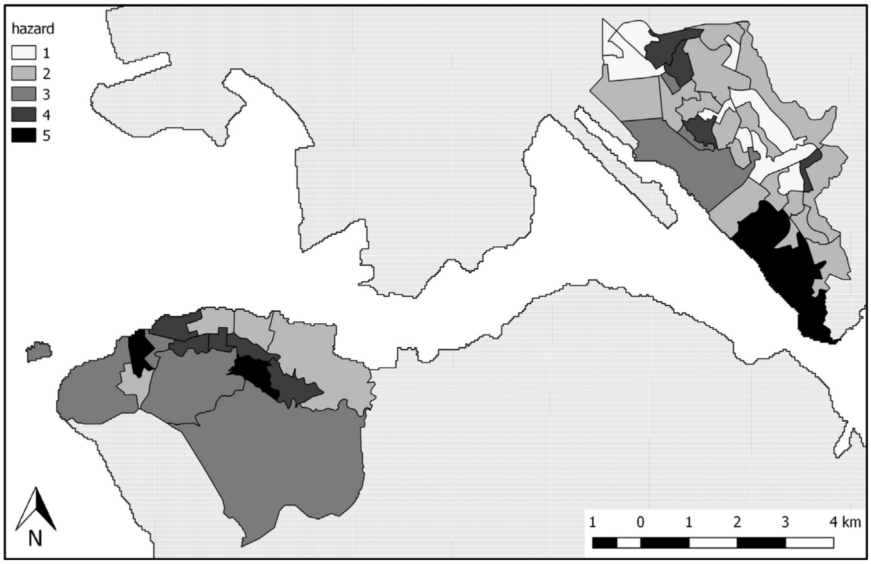

Fig. 5. Integrated hazards map for Central and Western District (left) and Kwun Tong District (right).

and represents an outlier (see Fig. 6a). As expected, Kwun Tong shows higher degrees of susceptibility to the three hazards due to the lower socio-economic status of its population (Fig. 6b). The coping capacity presents high vulnerability levels in Central and Western District due to the widespread one household arrangement mainly occupied by foreign housekeepers working and living in the wealthy district (Fig. 6c). Overall, Kwun Tong District shows higher vulnerability levels than Central and Western District.

From our calculations, all of Central and Western District's constituencies face the lowest vulnerability level of 1. As for Kwun Tong District's constituencies, nearly 75% have a vulnerability index of 1.

5.3. Multi-hazard risk

Relative to all other constituencies considered, the constituency Sau Mau Ping Central in Kwun Tong District faces the greatest multi-hazard risk; the most at risk constituency in Central and Western is Castle Road, which has the fourth highest risk level overall (see Fig. 8). Based on classifications using the equal interval ranking method, none of Central and Western District's constituencies face a risk level of 5 or 4. As for Kwun Tong's constituencies, 2 have a risk index of 5, and 1 is at level 4, while most are at level 1 or 2. To note is that risk levels are distributed across both districts showing that both face potential hazards impacts. The steps of our analysis allowed us to trace back the causes of risk showing how in the wealthier and less densely populated Central Western District higher hazards levels are to bale for considerable risk levels, while in Kwun Tong District high levels of hazard but especially susceptibility give rise to high levels of risk.

Looking at the constituencies ranking highest in terms of risk, three with the highest risk levels are located in Kwun Tong District while two are in Central and Western District. For hazard, two constituencies from Central and Western District have the highest hazard levels. The top nine most vulnerable constituencies are all located in Kwun Tong District.

6. Discussion

By performing a multi-hazard risk assessment using indicators, we identified particular areas within the two districts that show higher multi-hazard and vulnerability levels than others. Referring to the multi-hazard assessment, many of the constituencies of the Central and Western District presented high degrees of potential impact, being particularly exposed to the hazards considered despite being less dense and wealthier. The most vulnerable areas are characterised mainly by higher population densities and lower socio-economic indices in Kwun Tong. Integrating the multi-hazard index with the vulnerability score we find that the two districts have more comparable and distributed levels of risk, but as mentioned, these can be traced back to different causes – one being physical exposure and the other being socio-economic. Overall, the results of the multi-hazard risk assessment show that although both study areas are significantly exposed to multiple hazards, the most vulnerable communities are located in the less wealthy district.

It should be noted that these results are dependent on the weighting and aggregation techniques used. Whereas equal weights were utilized in this assessment, a more comprehensive weighting of hazards and aspects of vulnerability would require collaboration with stakeholders in order to define relations between the single hazard and vulnerability levels as they relate also to specific policy goals. An approach based on equal weighting nevertheless provides useful information for a comparative assessment of risk to multiple hazards in different areas of a city, as it highlights local concentration of those physical and socio-economic conditions that can determine elevated levels of risk. Nevertheless, a first screening aiming at the identification of place related vulnerabilities throughout the entire urban area can be useful for identifying those areas where vulnerabilities could be reduced using specific localized urban planning strategies. These strategies include, for example, increase of canopy and albedo (urban greening and accurate choice of surface materials), or increasing air circulation and reducing waste heat (creation of wind corridors, use of combined green and blue areas, and avoiding street canons) [84,85].

6.1. Climate change and socio-economic change implications for multi-hazard risk

Climate change scenarios for the region depict increasing impacts from heatwaves, extreme rainfall events, sea level rise, and droughts [49,86]. According to the 2015 Hong Kong Climate Change Report, climate change will lead to more very hot days and hot nights, fewer rainy days but increased average rainfall

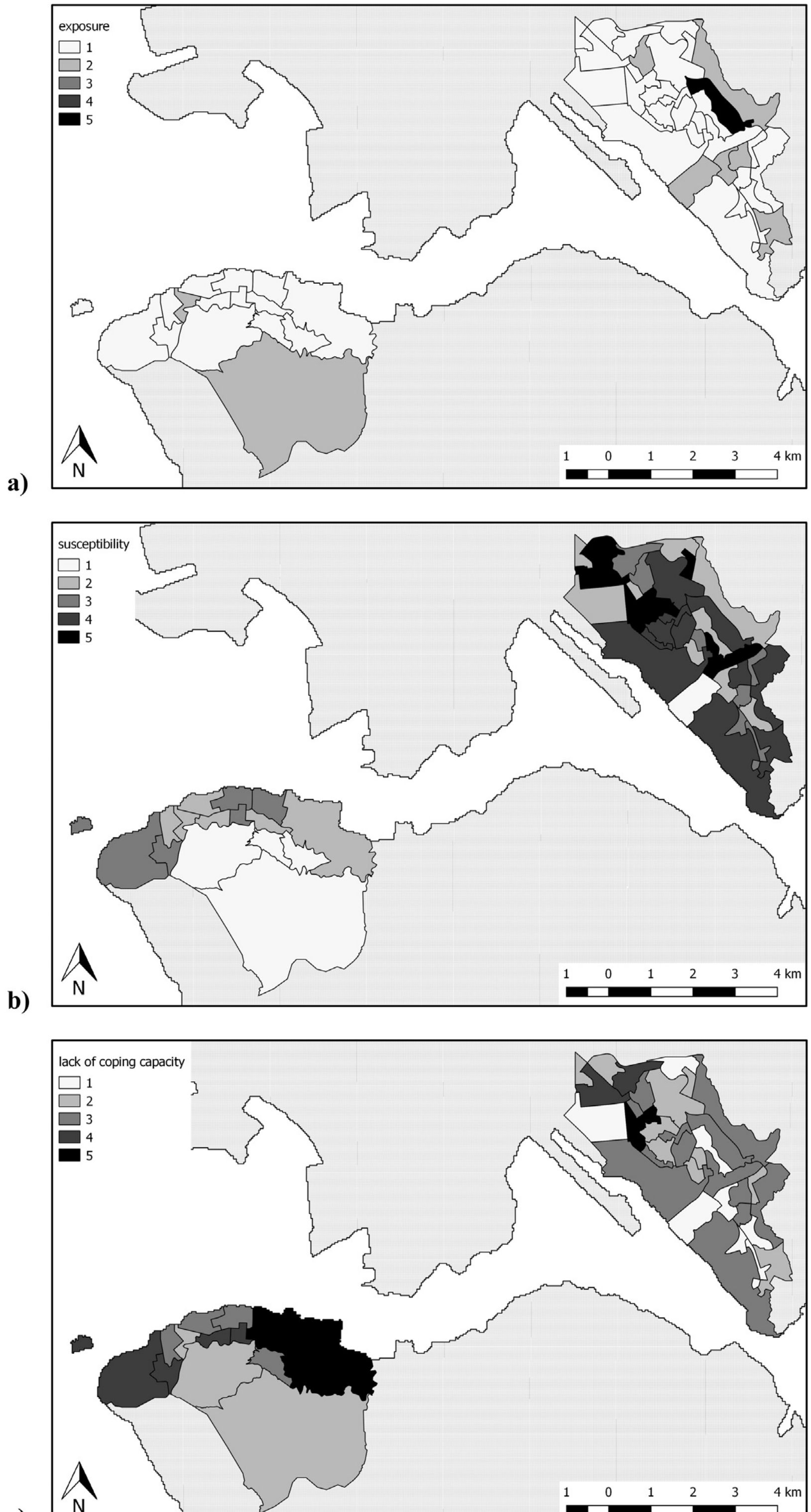

Fig. 6. (a) Exposure, (b) susceptibility, and (c) lack of coping capacity maps for Central and Western District (left) and Kwun Tong District (right).

intensity, more extreme rainfall events, more extremely wet years with risk of extremely dry years, global sea level rise will lead to coastal changes, and increased threat of storm surges associated with tropical cyclones [86]. According to tide gauge data maintained by the HKO, mean sea level in Victoria Harbor has already been increasing at a rate of 30 mm per decade from 1954 to 2014. Projected changes in mean sea level in Hong Kong by 2100 developed by the city, relative to the 1986–2005 average, range from 62 to 70–73 to 91 cm depending on the climate change scenario.

Sea level rise is an important factor to be considered in assessing the future development of hazard intensities. This might lead to further increasing hazard impacts also in the wealthiest parts of the city, which occupy low-lying areas and have already shown high levels of potential multi-hazard impacts. As it is for other coastal cities, such as New York, New Orleans, and London, mixed green and grey approaches could provide the necessary protection

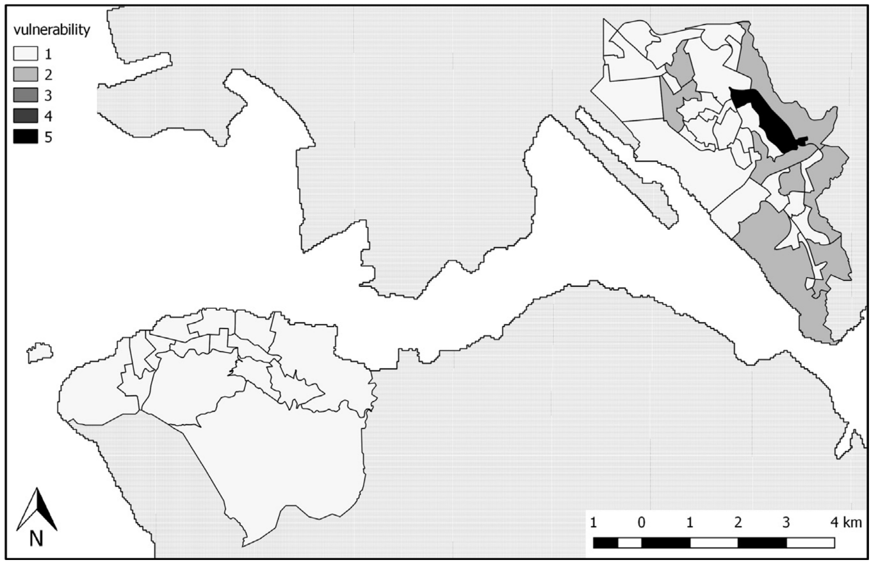

Fig. 7. Vulnerability map for Central and Western District (left) and Kwun Tong District (right).

to coastal flood while having the benefit of reducing the UHI effect at the same time. A multi-hazard approach allows for the detection of risk hotspots in cities for which multifunctional solutions could benefit at the reduction of risk to multiple hazards at once.

These climatic changes nevertheless would not modify the distribution of risk across the city in a significant way. Spatial patterns would not change significantly with exception of the risk of coastal flooding. So, in absence of spatially explicit projections of changes in the distribution of the socio-economic characteristics of the population, an additional mapping exercise would not yield new insights.

On the demographic side, the fertility rate in Hong Kong has been consistently below the replacement rate of 2.1, reaching approximately 1.2 in 2011 [42]. In contrast, life expectancy has increased and the proportion of the population aged 65 and over is projected to rise markedly, from 13% in 2011 to 30% in 2041, as also shown by the projected rising median age [42]. The ageing process of the society resulting from these phenomena will cause additional concerns for vulnerability reduction.

7. Conclusions

The spatial mapping of single and composite indicators is a powerful tool for directing future investigation to be focussed on particularly at risk areas. Policy action will need to address these fragilities, which have become evident both in the sense of reducing exposure in higher income neighbourhoods and focussing more attentively in improving susceptibility and coping capacities of populations in lower income and more densely inhabited areas of the city. Furthermore, this method allows for the identification of hotspots of risk where green or grey infrastructures might be the most needed.

Based on the methods of assessment employed herein, the integrated risk is highest where spatial intensity of hazards and vulnerability coincide. This is the case in some constituencies of Kwun Tong, where population density and susceptibility due to socio-economic factors are high, alongside with some medium to high hazard indices. A similar risk due to hazards exposure affects constituencies in Central and Western District where lower levels of vulnerability are encountered. As this analysis focuses essentially on the residential population, a specific vulnerability

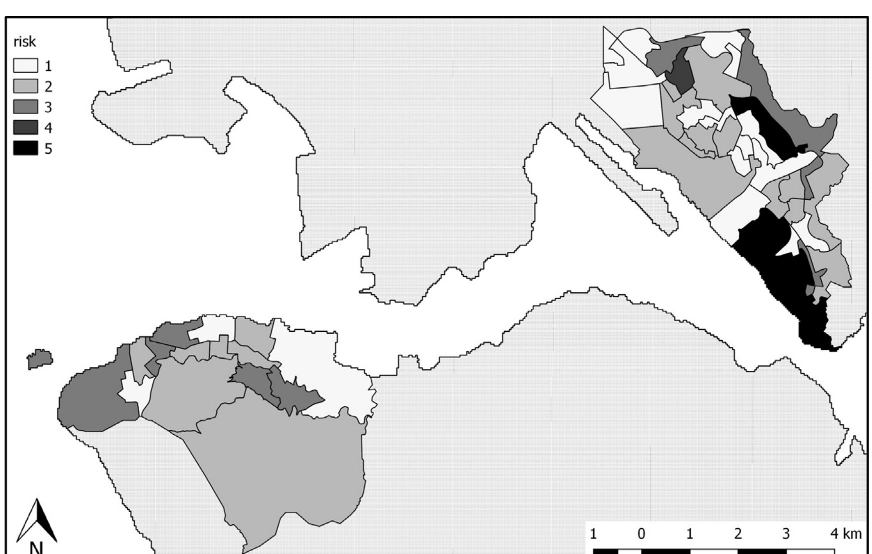

Fig. 8. Multi-hazard risk map for Central and Western District (left) and Kwun Tong District (right).

assessment with regards to working populations might suggest differentiated measures with respect to those targeting the residential population.

In summary, our analysis shows that under a multi-hazard risk approach, no parts of the two districts are significantly less exposed to multiple hazards than others. Nevertheless, elements contributing to higher or lower risk levels are not equally distributed across the city. In those areas where socio-economic factors drive or accentuate the overall risk level, improvements specifically addressing the socio-economic conditions of the population (like in most of the constituencies of Kwun Tong) and providing targeted services to improve coping capacity may be appropriate, whereas in others (like Central and Western) exposure reduction would be a more effective strategy. This leads to the conclusion that a multi-hazard risk assessment at the smaller scale is effective in identifying spatial distribution of principle drivers of risk that might change within a city and helps prioritizing interventions within different districts, at the very local level.

Acknowledgements

The research leading to these results has received funding from the Italian Ministry of Education, University and Research and the Italian Ministry of Environment, Land and Sea under the GEMINA project.

LiDAR data have been provided for use in this research project by the Hong Kong Civil Engineering and Development Department.

We would like to thank Francesco Bosello and two anonymous reviewers for their comments and helpful suggestions on a first draft of this paper.

References

[1] ESCAP, Overview of Natural Disasters and their Impacts in Asia and the Pacific, 1970–2014, Disaster Risk Reduction Section ICT and Disaster Risk Reduction Division, Economic and Social Commission for Asia and the Pacific (ESCAP), 2015.
[2] UNISDR, The Global Assessment Report on Disaster Risk Reduction (GAR) 2015. Making Development Sustainable: The Future of Disaster Risk Management, United Nations, 2015.
[3] UN, World Urbanization Prospects: The 2014 Revision: Highlights, United Nations Department of Economics and Social Affairs, Population Division, New York, 2014.
[4] IPCC, Climate change, Impacts, Adaptation, and Vulnerability. Part B: Regional Aspects. Contribution of Working Group II to the Fifth Assessment Report of the Intergovernmental Panel on Climate Change, Cambridge University Press, Cambridge U.K and New York, USA, 2014, 2014.
[5] E. Dickson, J.L. Baker, D. Hoornweg, A. Tiwari, Weltbank, eds., Urban risk assessments: understanding disaster and climate risk in cities, World Bank, Washington, DC, 2012.
[6] L. Filleul, S. Cassadou, S. Médina, P. Fabres, A. Lefranc, D. Eilstein, A. Le Tertre, L. Pascal, B. Chardon, M. Blanchard, C. Declercq, J.F. Jusot, H. Prouvost, M. Ledrans, The relation between temperature, ozone, and mortality in nine French cities during the heat wave of 2003, Environ. Health Perspect. 114 (2006) 1344–1347, http://dx.doi.org/10.1289/ehp.8328.
[7] R.J. Fuchs, Cities at risk: Asia's coastal cities in an age of climate change, East-West Centre, Honolulu, 2010.
[8] C. Wamsler, E. Brink, C. Rivera, Planning for climate change in urban areas: from theory to practice, J. Clean. Prod. 50 (2013) 68–81, http://dx.doi.org/10.1016/j.jclepro.2012.12.008.
[9] UNISDR, Proposed Updated Terminology on Disaster Risk Reduction: A Technical Review, The United Nations Office for Disaster Risk Reduction (UNISDR), 2015.
[10] J. Birkmann, ed., Measuring vulnerability to natural hazards: towards disaster resilient societies, United Nations University Press, Tokyo, New York, Paris, 2006. http://archive.unu.edu/unupress/sample-chapters/1135-MeasuringVulnerabilityToNaturalHazards.pdf.
[11] T.W. Collins, Marginalization, facilitation, and the production of unequal risk: the 2006 Paso del Norte floods, Antipode 42 (2010) 258–288, http://dx.doi.org/10.1111/j.1467-8330.2009.00755.x.
[12] IPCC, Managing the Risks of Extreme Events and Disasters to Advance Climate Change Adaptation (SREX), Cambridge University Press, Cambridge, UK and New York, NY, USA, 2012.
[13] M.L. Parry, O.F. Canziani, J.P. Palutikof, J.P. van der Linden, C.E. Hanson, eds., Climate Change 2007: Impacts, Adaptation and Vulnerability. Contribution of Working Group II to the Fourth Assessment Report of the Intergovernmental Panel on Climate Change Appendix, Cambridge University Press, Cambridge, UK, 2007.
[14] IPCC, Annex II Glossary, (2014). http://www.ipcc.ch/pdf/assessment-report/ar5/wg2/WGIIAR5-AnnexII_FINAL.pdf.
[15] P.H. Fischer, B. Brunekreef, E. Lebret, Air pollution related deaths during the 2003 heat wave in the Netherlands, Atmos. Environ. 38 (2004) 1083–1085, http://dx.doi.org/10.1016/j.atmosenv.2003.11.010.
[16] I. Preston, N. Banks, K. Hargreaves, A. Kazmierczak, K. Lucas, R. Mayne, C. Downing, R. Street, Climate change and social justice: an evidence review, Joseph Rowntree York, 2014. http://www.cse.org.uk/app/webroot/downloads/file/climate%20change%20and%20social%20justice%20evidence%20review.pdf.
[17] D. Satterthwaite, S. Huq, H. Reid, M. Pelling, P. Romero Lankao Adapting to climate change in urban areas: the possibilities and constraints in low and middle income nations, International Institute for Environment and Development (IIED), 2007.
[18] UNEP, Agenda 21. Tech. rep., United Nations Environment Programme, 1992.
[19] UN, Johannesburg Declaration on Sustainable Development. Plan of Implementation of the World Summit on Sustainable Development, United Nations; World Summit on Sustainable Development (UN), 2002.
[20] UNISDR, Hyogo Declaration, 2005.
[21] UNISDR, Sendai Framework for Disaster Risk Reduction 2015–2030, United Nations Office for Disaster Risk Reduction (UNISDR), Geneva, Switzerland, 2015.
[22] T. Tarvainen, J. Jarva, S. Greiving, Spatial pattern of hazards and hazard interactions in Europe, Spec. Pap. -Geol. Surv. Finl. 42 (2006) 83.
[23] W. Marzocchi, European Commission, Directorate General for Research, Principles of multi-risk assessment: interaction amongst natural and man-induced risks, EUR-OP, Luxembourg, 2009.
[24] M.S. Kappes, M. Keiler, T. Glade, Consideration of Hazard Interactions in Medium-Scale Multi-Hazard Risk Analyses, in: EGU Gen. Assem. Conf. Abstr., 2010: p. 3331. http://adsabs.harvard.edu/abs/2010EGUGA.12.3331K.
[25] A. Carpignano, E. Golia, C. Di Mauro, S. Bouchon, J.P. Nordvik, A methodological approach for the definition of multi-risk maps at regional level: first application, J. Risk Res. 12 (2009) 513–534.
[26] G. Hufschmidt, T. Glade, Vulnerability analysis in geomorphic risk assessment, Geomorphol. Hazards Disaster Prev. (2010) 233.
[27] M.S. Kappes, M. Keiler, K. von Elverfeldt, T. Glade, Challenges of analyzing multi-hazard risk: a review, Nat. Hazards 64 (2012) 1925–1958, http://dx.doi.org/10.1007/s11069-012-0294-2.
[28] M. Papathoma-Köhle, M. Kappes, M. Keiler, T. Glade, Physical vulnerability assessment for alpine hazards: state of the art and future needs, Nat. Hazards 58 (2011) 645–680, http://dx.doi.org/10.1007/s11069-010-9632-4.
[29] W. Marzocchi, A. Garcia-Aristizabal, P. Gasparini, M.L. Mastellone, A. Di Ruocco, , Basic principles of multi-risk assessment: a case study in Italy, Nat. Hazards 62 (2012) 551–573, http://dx.doi.org/10.1007/s11069-012-0092-x.
[30] M.S. Kappes, M. Papathoma-Köhle, M. Keiler, Assessing physical vulnerability for multi-hazards using an indicator-based methodology, Appl. Geogr. 32 (2012) 577–590, http://dx.doi.org/10.1016/j.apgeog.2011.07.002.
[32] S. Greiving, M. Fleischhauer, J. Lückenkötter, A Methodology for an integrated risk assessment of spatially relevant hazards, J. Environ. Plan. Manag. 49 (2006) 1–19, http://dx.doi.org/10.1080/09640560500372800.
[33] M. Dilley, Natural disaster hotspots: a global risk analysis, World Bank, Washington, D.C., 2005.
[34] S. Greiving, Multi-risk assessment of Europe's regions, in: J. Birkmann (Ed.), Meas. Vulnerability Nat. Hazards Disaster Resilient Socpp. 210–226, 2006.
[35] T. Welle, J. Birkmann, The world risk index – an approach to assess risk and vulnerability on a global scale, J. Extrem. Events 2 (2015) 1550003, http://dx.doi.org/10.1142/S2345737615500037.
[36] S. Kienberger, S. Lang, P. Zeil, Spatial vulnerability units – expert-based spatial modelling of socio-economic vulnerability in the Salzach catchment, Austria, Nat. Hazards Earth Syst. Sci. 9 (2009) 767–778, http://dx.doi.org/10.5194/nhess-9-767-2009.
[37] M.-L. Carreño, O.D. Cardona, A.H. Barbat, Urban Seismic Risk Evaluation: A Holistic Approach, Nat. Hazards 40 (2007) 137–172, http://dx.doi.org/10.1007/s11069-006-0008-8.
[38] K. Granger, T. Jones, M. Leiba, G. Scott, Community risk in Cairns, A multi-hazard risk assessment., The Australian Geological Survey Organisation (AGSO), Canberra, 1999.
[39] M. MiddelmannK. Granger, Community risk in Gladstone a multi-hazard risk assessment, Australian Geological Survey Organisation (AGSO), Cities Project, Canberra, 2000.
[40] Z.E.A. El Morjani, S. Ebener, J. Boos, E. Abdel Ghaffar, A. Musani, Modelling the spatial distribution of five natural hazards in the context of the WHO/EMRO Atlas of Disaster Risk as a step towards the reduction of the health impact related to disasters, Int. J. Health Geogr. 6 (2007) 8, http://dx.doi.org/10.1186/1476-072X-6-8.
[41] F.S. Ching, The population of Hong Kong, Committee for International Coordination of National Research in Demography (CICRED), Committee for International Cooperation in National Research in Demography, Paris, 1974.
[42] HK GOV, Hong Kong Population Projections 2012-2041, Demographic Statistics

Section, Census and Statistics Department, The Government of Hong Kong Special Administrative Region, 2012.
[43] W.B. Goggins, E.Y.Y. Chan, E. Ng, C. Ren, L. Chen, Effect modification of the association between short-term meteorological factors and mortality by urban heat islands in Hong Kong, PLoS ONE 7 (2012) e38551, http://dx.doi.org/10.1371/journal.pone.0038551.
[44] C. Lam, The weather aspect of disaster planning and preparedness in Hong Kong, in: Hong Kong, China, 2004.
[45] A.Y. Loke, C.K. Lai, O.W.M. Fung, At-home disaster preparedness of elderly people in Hong Kong: Disaster preparedness of elderly, Geriatr. Gerontol. Int. 12 (2012) 524–531, http://dx.doi.org/10.1111/j.1447-0594.2011.00778.x.
[46] P.H. Chau, K.C. Chan, J. Woo, Hot weather warning might help to reduce elderly mortality in Hong Kong, Int. J. Biometeorol. 53 (2009) 461–468, http://dx.doi.org/10.1007/s00484-009-0232-5.
[47] G. Brücker, Vulnerable populations: lessons learnt from the summer 2003 heat waves in Europe, Eur. Surveill. 10 (2005) 147.
[48] K.M.A. Gabriel, W.R. Endlicher, Urban and rural mortality rates during heat waves in Berlin and Brandenburg, Germany, Environ. Pollut. 159 (2011) 2044–2050, http://dx.doi.org/10.1016/j.envpol.2011.01.016.
[49] T. Kosatsky, The 2003 European heat waves, Eurosurveillance 10 (2005) 148.
[50] X.F. Huang, J.Z. Yu, Z. Yuan, A.K.H. Lau, P.K.K. Louie, Source analysis of high particulate matter days in Hong Kong, Atmos. Environ. 43 (2009) 1196–1203, http://dx.doi.org/10.1016/j.atmosenv.2008.10.013.
[51] K. Lam, T. Wang, C. Wu, Y. Li, Study on an ozone episode in hot season in Hong Kong and transboundary air pollution over Pearl River Delta region of China, Atmos. Environ. 39 (2005) 1967–1977, http://dx.doi.org/10.1016/j.atmosenv.2004.11.023.
[52] F.C. Dai, C.F. Lee, J. Li, Z.W. Xu, Assessment of landslide susceptibility on the natural terrain of Lantau Island, Hong Kong, Environ. Geol. 40 (2001) 381–391, http://dx.doi.org/10.1007/s002540000163.
[53] W.S. Yim, Vulnerability and adaptation of Hong Kong to hazards under climatic change conditions, Water Air Soil Pollut. 92 (1996) 181–190, http://dx.doi.org/10.1007/BF00175564.
[54] H. Lam, M.H. Kok, K.K.Y. Shum, Benefits from typhoons – the Hong Kong perspective, Weather 67 (2012) 16–21, http://dx.doi.org/10.1002/wea.836.
[55] F.C. Dai, C.F. Lee, L.G. Tham, K.C. Ng, W.L. Shum, Logistic regression modelling of storm-induced shallow landsliding in time and space on natural terrain of Lantau Island, Hong Kong, Bull. Eng. Geol. Environ. 63 (2004) 315–327, http://dx.doi.org/10.1007/s10064-004-0245-6.
[56] F.C. Dai, C.F. Lee, Landslide characteristics and slope instability modeling using GIS, Lantau Island, Hong Kong, Geomorphology 42 (2002) 213–228, http://dx.doi.org/10.1016/S0169-555X(01)00087-3.
[57] C.H. Zhou, C.F. Lee, J. Li, Z.W. Xu, On the spatial relationship between landslides and causative factors on Lantau Island, Hong Kong, Geomorphology 43 (2002) 197–207, http://dx.doi.org/10.1016/S0169-555X(01)00130-1.
[58] X. Yao, L.G. Tham, F.C. Dai, Landslide susceptibility mapping based on Support Vector Machine: A case study on natural slopes of Hong Kong, China, Geomorphology 101 (2008) 572–582, http://dx.doi.org/10.1016/j.geomorph.2008.02.011.
[59] K.T. Chau, J.E. Chan, Regional bias of landslide data in generating susceptibility maps using logistic regression: Case of Hong Kong Island, Landslides 2 (2005) 280–290, http://dx.doi.org/10.1007/s10346-005-0024-x.
[60] N.C. Evans, S.W. Huang, J.P. King, The natural terrain landslide study—phases I and II. Special project report SPR5/97, Geotech. Eng. Off. Hong Kong, 1997.
[61] K.T. Chau, Y.L. Sze, M.K. Fung, W.Y. Wong, E.L. Fong, L.C.P. Chan, Landslide hazard analysis for Hong Kong using landslide inventory and GIS, Comput. Geosci. 30 (2004) 429–443, http://dx.doi.org/10.1016/j.cageo.2003.08.013.
[62] G. Delmonaco, C. Margottini, D. Spizzichino, ARMONIA methodology for multi-risk assessment and the harmonisation of different natural risk maps, in: 2010-07-19 2014-11-07 Httpforum Eionet Eur. Eueionet-Air-Clim.-NIA-PROJECTDeliverable 2031 1 Pdf, 2006.
[63] K. Hewitt, I. Burton, Hazardousness of a place: a regional ecology of damaging events, 1971.
[64] QGIS, Development Team, QGIS Geographic Information System, Open Source Geospatial Foundation, 2009.
[65] Y. Depietri, T. Welle, F.G. Renaud, Social vulnerability assessment of the Cologne urban area (Germany) to heat waves: links to ecosystem services, Int. J. Disaster Risk Reduct. 6 (2013) 98–117, http://dx.doi.org/10.1016/j.ijdrr.2013.10.001.
[66] D. Haase, N. Schwarz, M. Strohbach, F. Kroll, R. Seppelt, Synergies, trade-offs, and losses of ecosystem services in urban regions: an integrated multiscale framework applied to the Leipzig-Halle region, Germany, Ecol. Soc. (2012), http://dx.doi.org/10.5751/ES-04853-170322.
[67] N. Larondelle, D. Haase, N. Kabisch, Mapping the diversity of regulating ecosystem services in European cities, Glob. Environ. Change 26 (2014) 119–129, http://dx.doi.org/10.1016/j.gloenvcha.2014.04.008.
[68] M. Damm, Mapping Social-Ecological Vulnerability to Flooding-a sub-national approach for Germany, Universitäts-und Landesbibliothek Bonn, 2010.
[69] T. Welle, Y. Depietri, M. Angignard, J. Birkmann, F. Renaud, S. Greiving, Vulnerability Assess. Heat. Waves, Floods, Earthq. Using MOVE Framew.: Test. Case Cologne, Ger., Assess. Vulnerability Nat. Hazards Eur. Perspect. 97 (2014) 91.
[70] J. Birkmann, O.D. Cardona, M.L. Carreño, A.H. Barbat, M. Pelling, S. Schneiderbauer, S. Kienberger, M. Keiler, D. Alexander, P. Zeil, T. Welle, Framing vulnerability, risk Soc. Response.: MOVE Framew., Nat. Hazards 67 (2013) 193–211, http://dx.doi.org/10.1007/s11069-013-0558-5.
[71] M.A. McGeehin, M. Mirabelli, The potential impacts of climate variability and change on temperature-related morbidity and mortality in the United States, Environ. Health Perspect. 109 (2001) 185.
[72] M. Uzielli, F. Nadim, S. Lacasse, A.M. Kaynia, A conceptual framework for quantitative estimation of physical vulnerability to landslides, Eng. Geol. 102 (2008) 251–256, http://dx.doi.org/10.1016/j.enggeo.2008.03.011.
[73] J. Yardley, R.J. Sigal, G.P. Kenny, Heat health planning: The importance of social and community factors, Glob. Environ. Change 21 (2011) 670–679, http://dx.doi.org/10.1016/j.gloenvcha.2010.11.010.
[74] S. Lin, D. Shaw, M.-C. Ho, Why are flood and landslide victims less willing to take mitigation measures than the public? Nat. Hazards, 44, (2008) 305–314, http://dx.doi.org/10.1007/s11069-007-9136-z.
[75] G. O'Hare, S. Rivas, The landslide hazard and human vulnerability in La Paz City, Bolivia, Geogr. J. 171 (2005) 239–258, http://dx.doi.org/10.1111/j.1475-4959.2005.00163.x.
[76] E. Frankenberg, B. Sikoki, C. Sumantri, W. Suriastini, D. Thomas, Education, Vulnerability, and Resilience after a Natural Disaster, Ecol. Soc. (2013), http://dx.doi.org/10.5751/ES-05377-180216.
[77] S.L. Harlan, J.H. Declet-Barreto, W.L. Stefanov, Neighborhood Effects on Heat Deaths: Social and Environmental Predictors of Vulnerability in Maricopa County, Arizona, Environ. Health Perspect. 121 (2012) 197–204, http://dx.doi.org/10.1289/ehp.1104625.
[78] Y.J. Lee, Social vulnerability indicators as a sustainable planning tool, Environ. Impact Assess. Rev. 44 (2014) 31–42, http://dx.doi.org/10.1016/j.eiar.2013.08.002.
[79] C. Ni, M.C.M. Chow, X. Jiang, S. Li, S.M.C. Pang, Factors Associated with Resilience of Adult Survivors Five Years after the 2008 Sichuan Earthquake in China, PLOS One. 10 (2015) e0121033, http://dx.doi.org/10.1371/journal.pone.0121033.
[80] A. Bouchama, Prognostic Factors in Heat Wave–Related Deaths < subtitle > A Meta-analysis < /subtitle> Arch. Intern. Med 167 (2007) 2170, http://dx.doi.org/10.1001/archinte.167.20.ira70009.
[81] A. Fouillet, G. Rey, F. Laurent, G. Pavillon, S. Bellec, C. Guihenneuc-Jouyaux, J. Clavel, E. Jougla, D. Hémon, Excess mortality related to the August 2003 heat wave in France, Int. Arch. Occup. Environ. Health 80 (2006) 16–24, http://dx.doi.org/10.1007/s00420-006-0089-4.
[82] M. Naughton, Heat-related mortality during a 1999 heat wave in Chicago, Am. J. Prev. Med. 22 (2002) 221–227, http://dx.doi.org/10.1016/S0749-3797(02)00421-X.
[83] G. Bankoff, G. Frerks, D. Hilhorst, s, development, and people, Mapping vulnerability: disaster, Earthscan Publications Ltd, London; Sterling, VA, 2004.
[84] B. Fernandez Milan, F. Creutzig, Reducing urban heat wave risk in the 21st century, Open Issue . 14 (2015) 221–231, http://dx.doi.org/10.1016/j.cosust.2015.08.002.
[85] M.S. O'Neill, R. Carter, J.K. Kish, C.J. Gronlund, J.L. White-Newsome, X. Manarolla, A. Zanobetti, J.D. Schwartz, Preventing heat-related morbidity and mortality: New approaches in a changing climate, Maturitas 64 (2009) 98–103, http://dx.doi.org/10.1016/j.maturitas.2009.08.005.
[86] Hong Kong Environment Bureau, Hong Kong Climate Change Report 2015, 2015.
[87] HK GOV, Hong Kong Population Census, 2011. Census and Statisticts Department, The Government of Hong Kong Special Administrative Region.